Multi-Neuromodulator Measurements across Fronto-Striatal Network Areas of the Behaving Macaque using Solid-Phase Microextraction

Seyed-Alireza Hassani[1,2,†] , Sofia Lendor[3,†] , Ezel Boyaci[3], Janusz Pawliszyn[3,‡,*], and Thilo Womelsdorf[1,2,‡,*]

1 Department of Psychology, Vanderbilt University, PMB 407817, 2301 Vanderbilt Place, Nashville TN 37240, USA
2 Department of Biology, Centre for Vision Research, York University, Toronto, Ontario M6J 1P3, Canada
3 Department of Chemistry, University of Waterloo, 200 University Avenue West, Waterloo, Ontario N2L 3G1, Canada

* Corresponding author 1: Tel. 519-888-4641, Fax. 519-746-0435, E-mail: janusz@uwaterloo.ca
* Corresponding author 2: Tel. 615-322-0070, E-mail: thilo.womelsdorf@vanderbilt.edu
† ‡ These authors contributed equally

Abstract

Different neuromodulators rarely act independent from each other to modify neural processes but are instead co-released, gated, or modulated. To understand this interdependence of neuromodulators and their collective influence on local circuits during different brain states, it is necessary to reliably extract local concentrations of multiple neuromodulators in vivo. Here we describe results using solid phase microextraction (SPME), a method providing sensitive, multi-neuromodulator measurements. SPME is a sampling method that is coupled with mass spectrometry to quantify collected analytes. Reliable measurements of glutamate, dopamine, acetylcholine and choline were made simultaneously within frontal cortex and striatum of two macaque monkeys (*Macaca mulatta*) during goal-directed behavior. We find glutamate concentrations several orders of magnitude higher than acetylcholine and dopamine in all brain regions. Dopamine was reliably detected in the striatum at tenfold higher concentrations than acetylcholine. Acetylcholine and choline concentrations were detected with high consistency across brain areas, within monkeys and between monkeys. These findings illustrate that SPME microprobes provide a versatile novel tool to characterize multiple neuromodulators across different brain areas in vivo to understand the interdependence and co-variation of neuromodulators during goal directed behavior. Such data will be important to better distinguish between different behavioral states and characterize dysfunctional brain states that may be evident in psychiatric disorders.

Introduction

Extracellular concentrations of neuromodulators influence firing regimes, input-output relationships and neural interactions in local circuits and long-range brain networks (Marder 2012; Thiele and Bellgrove 2018), and are dysregulated in virtually all psychiatric disorders (Avery and Krichmar 2017; Millan et al. 2012). Accumulating evidence suggests that these fundamental roles of neuromodulators for circuit functioning are unlikely realized by single neuromodulators operating in isolation. Rather, neuromodulatory systems are heavily intertwined (Avery and Krichmar 2017; Gobert et al. 1998; Moehle et al. 2017), and operate simultaneously on individual cells and circuits (Arnsten et al. 2010; Hassan et al. 2015; Marder 2012; Santana et al. 2018). In each circuit, local mechanisms exert control over the release of neuromodulators from terminals of brainstem-originating projection neurons. This local control proceeds through activation of pre-synaptic glutamatergic receptors (Ghersi et al. 2003; Grilli et al. 2009; Luccini et al. 2007; Pittaluga 2016; Pittaluga et al. 2006; Wang et al. 1992). These insights suggest that an understanding of the contribution of neuromodulators to circuit functioning requires measuring, simultaneously, multiple neuromodulators in conjunction with ongoing glutamatergic neurotransmitter concentrations and action. Consistent with this conclusion single neuromodulator theories often fail to account for all observable symptoms in psychiatric diseases (Bohnen et al. 2015; Halliday et al. 2014; Remy et al. 2005).

Despite the accumulating evidence for the interdependence of neuromodulator actions, few methods exist for their simultaneous measurement in vivo and across multiple brain areas (**Table S1**). Most of these existing neurochemical sensing methods have a high barrier to entry by requiring specialized equipment and trained experts preventing data collection by scientists who are otherwise interested in the role of endogenous and exogenous neuroactive chemicals in

61 cognition and psychiatric disorders. Electrochemical methods such as fast scan cyclic
62 voltammetry (FSCV) and amperometry have sub-second temporal resolution, but are limited to
63 the measurement of a few compounds (Dale et al. 2005; Jacobs et al. 2010) and are not robust for
64 in vivo application in nonhuman primates (Vartak et al. 2017). Imaging techniques such as
65 positron emission tomography (PET) are also limited to the measurement of one or a few
66 compounds simultaneously (Fisher et al. 1995). Microdialysis (MD) paired with mass
67 spectrometry is the most commonly used method for measuring multiple neuromodulators in
68 awake behaving animals. MD provides a data collection method which is then analyzed post hoc
69 to identify and quantify collected analytes. It operates with a semi-permeable membrane which
70 allows for the continuous collection of the available extracellular neuromodulators through
71 passive diffusion, and can even be used to locally release pharmacological agents (Anderzhanova
72 and Wotjak 2013; Kennedy 2013; Watson et al. 2006). However, MD does have several
73 disadvantages including disrupting the tissue during its initial placement of the probe or a
74 guiding cannula resulting in damage-induced release of neuromodulators that can last several
75 hours before stable measurements become possible. Moreover, MD has low affinity for
76 hydrophobic compounds and comparatively broad spatial and temporal resolution that is in the
77 range of 200-400 μm in diameter and 10-20 minutes, respectively. These values are dependent
78 on the surface area of the permeable membrane, the exact method of MD, flow rate, resolution of
79 detection methods for analytes of interest, tissue tortuosity and more (Anderzhanova and Wotjak
80 2013; Kennedy 2013; Watson et al. 2006).

81 In light of these limitations of available measurement techniques, we set out to
82 characterize a novel protocol for measuring multiple neuromodulators in vivo using probes
83 optimized for solid phase microextraction (SPME) (Pawliszyn 2012). SPME probes are thin (200

84 μm) wires of arbitrary length coated with an inert porous polymeric matrix using biocompatible
85 binder on one end where molecules with appropriate size and affinity migrate via passive
86 diffusion and are retained by chemical interactions (*see* Methods). SPME provides an alternate
87 method for data collection which can then be analyzed by tools such as mass spectrometers. This
88 method has been shown to extract in neural tissue dynamic changes in dopamine (DA) and
89 serotonin (5-HT) levels with comparable precision to MD (Cudjoe et al. 2013; Cudjoe and
90 Pawliszyn 2014). Additionally, due to the similarity of SPME probes to commonly used
91 microelectrodes in electrophysiological recordings, relatively minor adjustments will allow for
92 the adaptation of conventional microelectrode driving systems for SPME use. This, combined
93 with post collection analysis through standard chemistry facilities makes SPME an attractive and
94 easy-to-use tool for electrophysiology labs.

95 The ability of SPME to report major neuromodulators as well as glutamate and GABA
96 were tested in two behaving rhesus macaques. Probes were repeatedly and simultaneously
97 inserted into two cortical regions and the striatum to observe inter-areal differences between
98 extracellular neuromodulator concentrations. We found that extracellular concentrations of
99 glutamate, dopamine, acetylcholine and choline could be reliably distinguished and differed
100 systematically between brain regions.

101

102 **Methods**

103 **Animals**

104 Data was collected from two 8 year-old male rhesus macaques (*Macaca mulatta*) weighing 8-12
105 kg. All animal care and experimental protocols were approved by the York University Animal
106 Care Committee and were in accordance with the Canadian Council on Animal Care guidelines.

107 Details regarding the experimental setup, recording procedures, and reconstruction of recording
108 sites have been described previously (Oemisch et al. 2015). Briefly, animals were implanted with
109 a 20 mm by 28 mm recording chamber over the frontal region of the right hemisphere guided by
110 stereotaxic coordinates (Paxinos et al. 2000) and MR images. The animals were seated in a
111 custom made primate chair and head stabilized with their eyes 65cm away from a 21' LCD
112 monitor refreshed at 85 Hz. Eye traces were collected by a video-based eye-tracking system
113 (Eyelink 1000 Osgoode, Ontario, Canada, 500 Hz sampling rate). The animals were engaged in
114 an over-trained attention tasks in which they would use saccadic eye movements to acquire juice
115 reward. The specifics of the task are described elsewhere (Hassani et al. 2017). Both animals
116 showed stable performance and acquired similar reward volumes on all recording days. In both
117 tasks, stimulus presentation and reward delivery was controlled through MonkeyLogic
118 (http://www.brown.edu/Research/monkeylogic/).

119 **SPME protocol and Fabrication of SPME Probes**

120 We provide a visual overview of the complete SPME protocol used here in **Fig S1** and delineate
121 the chemical materials, LC-MS/MS analysis, and detailed quantitation of neuromodulators in the
122 ***Supplementary Methods*** and in a companion paper (Lendor et al., submitted). All measurements
123 used miniaturized SPME probes that were manufactured by repeated dip-coating of stainless
124 steel wires in a suspension of extracting phase in a binder. This general procedure reported
125 previously (Gómez-Ríos et al. 2017), has been modified to fit the purpose of *in vivo* brain
126 sampling (Lendor et al., submitted). The 3 mm long tip of the wire was acid-etched down to
127 approx. 100 μm to create a recession capable of accommodating thicker layer of coating without
128 significantly increasing the total probe diameter. The extracting phase was an in-house
129 synthesized hydrophilic-lipophilic balance polymer functionalized with benzenesulfonic acid to

130 introduce strong cation exchange properties (HLB-SCX). The monodispersed polymeric particles
131 with diameter of approx. 1 μm were suspended in the binder consisting of 7% polyacrylonitrile
132 dissolved in N,N-dimethylformide (w/v), ensuring the particles-to-binder ratio at 15% (w/v). The
133 extracting phase suspension was prepared one day before the probe coating, homogenized by
134 sonication and stirred at 800 rpm overnight. Several layers of coating were deposited on the
135 modified wires, resulting in total coating thickness of ≈50 μm and total probe diameter of 195
136 μm. The average pore size of the extracting phase was measured at 1.2nm. Before the use, the
137 probes were cleaned with the mixture of methanol, acetonitrile and 2-propanol (50:25:25, v/v/v),
138 activated in the mixture of methanol and water (50:50. v/v) and sterilized in steam for 15 min at
139 121°C. During the sampling, SPME probes were inserted into sheathing cannulas to protect the
140 coating and prevent it from extracting compounds on the way to the target brain area. The
141 cannulas underwent the same cleaning and sterilization procedure as the probes and then the
142 lengths of both components of the SPME assembly were adjusted to 60-70 and 70-80 mm for the
143 probes and cannulas, respectively.
144

145 **MRI Guided Electrophysiological Mapping of Target Tissue**

146 The anatomical coordinates of the brain regions of interest were first identified through 3 T MR
147 images. The MR images were then verified with extracellular electrophysiological recordings of
148 the target areas, which provided the gray and white matter boundaries for the cortical sites and
149 the dorsal most aspect of the head of the caudate nucleus. Tungsten microelectrodes were 200
150 μm thick with an impedance of 1-2 MΩ. All electrodes, SPME probes and their accompanying
151 guiding cannulas were driven down into the brain and later out using software-controlled
152 precision microdrives (Neuronitek, ON, Canada). Electrodes were connected to a multichannel

153 acquisition processor (Neuralynx Digital Lynx system, Inc., Bozeman, Montana, USA) which
154 was used for data amplification, filtering and acquisition of spiking activity. Spiking activity was
155 obtained by applying a 600-8000 Hz bandpass filter, with further amplification and digitization
156 at a 32 KHz sampling rate. For every recording day, electrodes were lowered until the first
157 detection of spiking activity (indicative of gray matter) at the depth suggested by the MR images.

158

159 **SPME Sampling and Post-Processing Procedures**

160 All three SPME assemblies (example of sampling using one assembly in **Fig 1A-C**) were
161 simultaneously driven to 200 μm above the point of first spiking detection. SPME assemblies
162 were located ~1 mm away from the electrode penetration location. Then, only the SPME probes
163 were inserted 3 mm into the areas of interest. On average macaque cortical thickness is only 2
164 mm while the head of the caudate at the point of sampling was well over 3 mm. An extraction
165 duration of 20 min was selected to reflect stable extraction time profiles for all compounds of
166 interest. Extraction time profiles reflect the detectable concentration of collected analyte over
167 time, which is captured in sequence by a linear "kinetic" regime, a "dynamic" regime and an
168 "equilibrium" regime over extraction time. We illustrate in **Fig 1D-E** these regimes for two main
169 compounds measured with the SPME probe we used in vivo. After the 20 min extraction event,
170 all SPME probes were driven back 3 mm into the guiding cannulas and all SPME assemblies
171 were withdrawn from the brain (**Fig 1A-C**).

172 The microdrives were removed from the chamber to enable unclamping of the SPME
173 probes, a brief wash and then storage in glass vials surrounded by dry ice until placing them into
174 a -80°C freezer. One entire sampling event (one extraction in 3 different brain areas together
175 with assembling the SPME probes and cannulas, driving into and out of brain, washing and

176 preparing for storage) was performed within 50 min, except for the first sampling event in each
177 sampling day. The first sampling event, with the area identification using electrophysiology
178 recording, was performed within 75 min.
179
180 **Neuromodulators detection and quantitation**
181 Detection and quantitiation of neuromodulators followed previously established procedures
182 described in the **Supplementary Material**. In brief, SPME probes were defrosted and desorbed
183 in an aqueous solution containing water, acetonitrile, methanol, formic acid and deuterated
184 isotopologues of target neuromodulators as internal standards (IS). Chromatographic separation
185 of target compounds was conducted as previously reported (Cudjoe and Pawliszyn 2014).
186 Tandem mass spectrometry (MS/MS) was performed with electrospray ionization with two
187 MS/MS transitions for each neuromodulator and one for each IS (Lendor et al., submitted).
188 Stock solutions of all target neuromodulators were prepared and used to generate
189 standard calibration curves and to calculate the amounts of neuromodulator extracted by each
190 experimental SPME probe. Conversion of the amount of neuromodulator extracted to in-brain
191 concentrations was done using matrix-matched external calibrations. LOD is defined as 3 times
192 the signal obtained from blank samples.
193
194 **Results**
195 During all measurements animals were engaged in a cognitively demanding task with stable
196 behavioral performance to minimize state dependent fluctuations of basal extracellular
197 concentrations of neuromodulators. Three brain regions were selected to provide a sample of
198 extracellular neuromodulatory concentrations. Two cortical regions: prefrontal cortex (PFC) area

199 8, premotor cortex (PreMC) area 6 and the head of the caudate nucleus (CD) were selected (**Fig**
200 **1F**). In 3 daily sessions, we sampled 3 times per session simultaneously from all three areas.
201 Monkey As had an additional 3 days of recording with one sample collected on each day.
202 Overall we collected and analyzed 12 probes in monkey As and 9 probes in monkey Ke. We
203 were specifically interested in major neuromodulators and neurotransmitters but successfully
204 measured other compounds such as amino acids (e.g. glutamine, taurine, phenylalanine etc) that
205 we do not discuss here.

206 To allow comparison of the SPME extraction results to those typically reported in
207 microdialysis studies, we calculated the relative change in measured concentrations across the
208 three successive sampling events per session pooled across monkeys to enhance the statistical
209 power of the analysis (**Fig 2**). Relative to the end of the first sampling event, the second and third
210 sampling events started after 40 minutes and 100 minutes respectively. We expected that the
211 variability of measurements (indexed as standard error of the median) is comparable to
212 repeatedly measured microdialysis of an identical, active brain state. We found that measured
213 concentrations did not change significantly across sampling events for any compound area
214 combination (Wilcoxon rank sum test; **Fig 2**).

215 We found that four target neurotransmitters and neuromodulators were reliably detected
216 in each animal: glutamate, dopamine, acetylcholine, and choline. Serotonin was also detected on
217 several probes but always near the limit of detection (LOD) and therefore was excluded from
218 analyses here (a report of serotonin is provided in the **Supplementary Results**) (Lendor et al.,
219 submitted). Glutamate concentrations were several orders of magnitude higher than all other
220 observed compounds of interest in all areas and both animals. Relative to glutamate, choline

221 concentrations were >15 times lower, DA concentrations were >700 lower and ACh
222 concentrations were >8300 times lower (**Fig 3**).

223 Glutamate concentrations (across areas), measured as median ± standard error, ranged
224 from 159,147 (±19,395) to 233,659 ng/mL (±33,917) in monkey As, and from 135,523
225 (±22,945) to 184,333 ng/mL (±33,516) in monkey Ke. Neither animal showed a significant
226 difference in glutamate concentrations between areas (As: kruskal-wallis test, p = 0.063; Ke:
227 kruskal-wallis test, p = 0.48). However, in both monkeys, glutamate concentrations were highest
228 in the head of the caudate, which showed a trend to be higher in the caudate than in premotor
229 cortex in monkey As (Wilcoxon rank sum test, p = 0.0226, not significant at the Bonferroni
230 corrected alpha level of p= 0.0167). Comparisons between monkeys showed no significant
231 differences between the glutamate concentrations in any of the measured areas (**Fig 3**).

232 In addition to glutamate, dopamine could be reliably detected in both monkeys in the
233 caudate at concentrations of 232 ng/mL (±47) in monkey As, and 226 ng/mL (±31) in monkey
234 As. These concentrations were similar between monkeys (Wilcoxon rank sum test p = 1, n.s.).
235 Dopamine was not found above detection limits in frontal cortex.

236 Acetylcholine measurements in the three brain areas ranged from (across areas) 25 (±2)
237 to 36 ng/mL (±5) in monkey As, and from 29 (±2) to 36 ng/mL (±4) in monkey Ke. Extracellular
238 ACh concentrations were significantly different between areas in monkey As (kruskal-wallis test,
239 p = 0.008). The caudate showed significantly higher concentrations than premotor cortex and a
240 trend to higher concentrations than PFC (PFC8a: Wilcoxon rank sum test, p = 0.04; PreM6:
241 Wilcoxon rank sum test, p = 0.005); only the difference between PreM6 and caudate survived
242 multiple comparisons correction (Bonferroni alpha = 0.0167). Cortical areas were not
243 significantly different from one another (Wilcoxon rank sum test, p = 0.17). In monkey Ke, only

244 one cortical region had concentrations of ACh above detection limits, which approached
245 significant difference to the concentrations measured in the caudate (Wilcoxon rank sum test, p =
246 0.08). Measurements of extracted ACh in the pre-motor cortex of monkey Ke were consistently
247 below detection limits (**Fig 3**).

248 We next measured choline which is a main product of the enzymatic breakdown of the
249 highly regulated ACh and which is a main indicator of attentional modulation of cholinergic
250 activity in frontal cortex (Parikh et al. 2007). Choline concentrations ranged across areas from
251 2,914 (±590) to 5,078 ng/mL (±675) in monkey As, and 3,408 (±3,705) to 5,533 ng/mL (±860)
252 in monkey Ke. Choline concentrations between areas were significantly different in monkey As
253 (kruskal-wallis test, p = 0.0262), but not monkey Ke (kruskal-wallis test, p = 0.25). Pairwise
254 comparisons in monkey As showed that concentrations after multiple comparison correction
255 were significantly different between PreM6 and the caudate (Wilcoxon rank sum test, p = 0.01;
256 Bonferroni alpha = 0.0167), and approached significance for PFC8 *versus* caudate (Wilcoxon
257 rank sum test, p = 0.06; Bonferroni alpha = 0.0167). Comparisons of choline concentrations
258 between monkeys were not significant in any of the measured areas.

259

260 **Discussion**

261 We demonstrated the reliable measurements of glutamate, dopamine, acetylcholine and choline
262 simultaneously within cortical and subcortical regions of awake and behaving macaques using
263 coated microprobes optimized for solid phase microextraction. Glutamate concentrations were
264 several orders of magnitude higher than dopamine, acetylcholine and choline across brain
265 regions. Extracellular concentrations of choline, dopamine and acetylcholine were detected at
266 >15, >700, and >8,300 times lower than glutamate respectively. Dopamine was readily detected

267 in the caudate but not observed at detectable concentrations in the cortical regions measured.
268 Acetylcholine concentrations showed a statistical trend of being different between the caudate
269 and measured cortical areas and with high consistency between monkeys. Choline
270 concentrations, a product of acetylcholine degradation as well as a precursor for its synthesis,
271 were negatively correlated with acetylcholine ($R = -0.355$; $p = 0.01$). Together, these findings
272 provide new and rare insights about the neurochemical circuit profiles during an active brain
273 state in three areas of the primate fronto-striatal network.

274 The high consistency of measured concentrations within animals, between brain areas
275 and between monkeys suggests that SPME microprobes could provide a versatile neuro-
276 technique for understanding how variations of the neurochemical milieu relate to local and long-
277 range circuit operations and ultimately cognitive functioning.

278

279 **Extracellular Concentrations of Glutamate, Dopamine, Acetylcholine and Choline.** Our
280 results revealed particularly high levels of glutamate within all measured brain regions (PFC,
281 PreMC, and CD) relative to other neuromodulators. This finding is consistent with its ubiquitous
282 role as major excitatory neurotransmitter. This holds true even in the caudate which consists
283 exclusively of GABAergic neurons, but receives glutamatergic inputs from the cortex (Haber
284 and Knutson 2010). Tonic concentrations of glutamate within the striatum have been previously
285 reported to be comparable to that of the hippocampus, prefrontal cortex and other cortical areas
286 due to glutamatergic inputs, extra-synaptic release and glial release (Ascenzo et al. 2006;
287 Moghaddam 1993; Moussawi et al. 2011). In contrast, classical neuromodulators such as DA and
288 ACh, are released in extracellular space through volume transmission where they are highly
289 regulated and may bind to receptors on multiple neurons (Santello et al. 2012; Schwartz and

290 Javitch 2013; Syková 2004; Vizi 2000). This regulation may help explain the relatively low
291 observed concentrations of DA and ACh and may be a large source of extracellular choline
292 through the enzymatic breakdown of ACh.

293 Extracellular DA was measured well above the detection threshold in the striatum. In
294 combination with glutamatergic and cholinergic concentrations, our results show promise in the
295 application of SPME to further our understanding of the relationship between glutamatergic
296 inputs to the striatum and the neuromodulatory ACh and DA signals impinging on striatal
297 circuits. Such circuits are strongly involved in hypo- and hyperkinetic diseases (Halliday et al.
298 2014; Millan et al. 2012). Dopaminergic signals did not exceed the detection threshold in either
299 cortical regions. The presence of DA in the PFC is well documented (Goldman-Rakic et al.
300 1990) and thus has failed to exceed our detection limit. A possible explanation for the lack of
301 detectable cortical DA is the susceptibility of catecholamines to oxidation. This may be partially
302 addressed by faster coupling of sample collection to quantitation by MS (see **Supplementary**
303 **Discussion**).

304 Few previous studies have documented ACh concentrations in vivo due to its rapid
305 breakdown by acetylcholinesterase (Kreitzer 2009; Schwartz and Javitch 2013; Zapata et al.
306 2013). ACh plays a major role in organizing local circuits, deployment of attention, locomotion
307 and reward through different receptors present in cortical and subcortical regions (Granger et al.
308 2016; Howe et al. 2017; Moehle et al. 2017). It has been difficult to discern which ACh
309 concentration corresponds to efficient endogenous circuit operations. Our finding of
310 measurements in all sampling locations except for premotor cortex in monkey Ke, is therefore a
311 promising starting point for future studies comparing ACh concentrations, in conjunction with
312 other neuromodulators, during different cognitive states. The fast turn-around of ACh due to

313 AChE however, likely leads to an underestimation of ACh concentrations by SPME. Although
314 AChE cannot traverse the porous SPME coating due to its size (~7.6nm diameter), preventing
315 any enzymatic degradation of trapped ACh (**Supplementary Material**), the dynamic
316 equilibration process continuously leads to a transfer of ACh out of the SPME coating following
317 the concentration gradient of the rapidly depleted ACh into the extracellular space as discussed
318 in the case of calibration in the coating approach (Alam and Pawliszyn 2016; Zhang et al.
319 2007a).

320 Amongst other sources, choline is created as a byproduct of ACh degradation by AChE.
321 Choline is also a precursor for the synthesis of ACh. Given this relationship, a negative
322 correlation between choline concentrations and ACh is expected which we indeed observed in
323 our dataset. Despite the difference in the measured concentrations of choline and acetylcholine,
324 other studies with similar differences have demonstrated the relationship of ACh and choline to
325 behavior within the cortex (Parikh et al. 2007). Future studies may focus on quantifying this
326 relationship across a wider range of brain states.

327

328 **Reliable Measurement of Individual Differences of State Specific Neuromodulatory Tone.**
329 Our results suggest that SPME probes provide reliable and sensitive measurements in
330 consecutive sampling events within an experimental session and between sessions on
331 consecutive days. These results were obtained while we controlled brain states across
332 measurement events by engaging animals in a cognitive task. This experimental control could
333 have contributed to the comparable extracellular levels of neuromodulators from sample to
334 sample within *and* between days from similar brain locations (**Fig 2**) (Marder et al. 2014;
335 McGinley et al. 2015; Reimer et al. 2014, 2016). The reproducibility of multiple measurements

336 at the same anatomical location within and between days suggests that the SPME penetrations
337 did not significantly disturb tissue (Cudjoe et al. 2013) (**Supplementary Information**). This
338 conclusion contrasts with reported experience from microdialysis measurements, where the
339 initial placement of the probe or guiding cannula causes transient measurement instabilities that
340 can require several hours of settling time before reliable, steady state neuromodulator
341 concentrations are measurable (Kodama et al. 2002, 2015, 2017; Moussawi et al. 2011;
342 Watanabe et al. 1997). These waiting periods must be taken into account when designing
343 microdialysis experiments for in vivo tracking of neuromodulators during behavioral tasks in
344 awake and restrained animals. Furthermore, the reliability of observations for the reported
345 neurochemicals with SPME is extremely high and outperforms many reported microdialysis
346 studies. We present 100% reliability in reporting glutamate and choline concentrations in all
347 brain regions and subjects. Acetylcholine concentrations were reported with 100% reliability in
348 one animal and 92% (11/12 probes) in the other within the prefrontal cortex, 0% reliability
349 (below detection threshold) in one animal and 83% (10/12 probes) in the other within the
350 premotor cortex and 100% reliability in one animal and 92% (11/12 probes) in the other within
351 the caudate. Dopamine concentrations were reported with 100% reliability in both animals in the
352 caudate and were not observed above detection thresholds in the cortex.
353
354 **Qualities and Advantages of SPME.** Our results illustrate several inherent advantages of using
355 SPME to measure neurochemical profiles in brain circuits (Lendor et al., submitted). As
356 illustrated in **Table S1**, SPME complements or outperforms alternative techniques in various
357 domains. Practically, the arbitrary length of the wire where the SPME coating is placed allows
358 for robust placement within the brain. The narrow diameter of the SPME probe that is within the

359 range common to electrodes for electrophysiological recordings, allows for repeated,
360 simultaneous sampling at multiple sites without observable changes to detected extracellular
361 neuromodulator levels using 20-minute sampling times.

362 *Spatial Resolution.* In principle, the spatial resolution of the SPME measurements are
363 capable of reflecting laminar concentration gradients across areas as small as several tens of
364 micrometers. In our protocol we coated 3mm in length with 50 μm of thickness and desorbed the
365 entire area into an organic solvent mixture for subsequent LC-MS/MS analysis. However, with
366 the use of other techniques, such as desorption electrospray ionization (DESI), which represents
367 a direct-to-MS approach (Deng et al. 2014), much smaller areas of the SPME matrix may be
368 analyzed at a time allowing for laminar or near-laminar resolution. Direct coupling of SPME
369 fibres to MS is the preferred mode, as it provides the most rapid analysis thus preventing
370 diffusion of compounds within the coating and smearing the imprinted layer information. If
371 diffusion of molecules within the fibre is high, it can be prevented by, for example, the inclusion
372 of a divider between two halves of the coating. This would allow the simultaneous measurement
373 of separated compartments of a cortical column. The absolute spatial resolution of SPME is
374 difficult to estimate as SPME operates through diffusion and dynamic equilibration similar to
375 MD. As a consequence, the sampled volume will depend on sampling time, the compound's
376 diffusion coefficient, as well as the target tissue and its properties affecting the rate of diffusion
377 such as tortuosity (Syková 2004).

378 *Temporal Resolution.* Several factors determine the appropriate extraction time using
379 SPME. Depending on the goals of an experimenter, resolutions below 5 minutes may be
380 achieved as the detection limit is reached within the first few minutes for most compounds tested
381 (**Fig 1D-E**). As sampling continues, the SPME coating will eventually reach an equilibrium point

382 with the external environment (**Fig 1D-E**). In principle, sampling times beyond a stable
383 equilibrium point will result in the same extracted values of compounds. However, in the brain
384 there is no single stable equilibrium point and thus, even with long sampling times, there will be
385 some variation in extracted concentrations. Within the dynamic regime, we can still calculate
386 environmental concentrations from which sampling occurred given knowledge of the extraction
387 time and the dynamic range. The lower limit of this dynamic range that can be informative is
388 determined by the coating's physicochemical characteristics and sample's properties and in
389 practice also volume of desorption and sensitivity of the MS. The analytical technique's
390 sensitivity also practically determines the thickness of the SPME coating as thinner coatings
391 could in principle increase temporal resolution but would extract less compounds overall
392 requiring higher sensitivity to detect. With higher sensitivity, less time is required for the thin
393 coating to extract sufficient amounts to exceed limits of detection and quantitation. This then
394 means that the compound with regards to which the sensitivity is the lowest, limits the temporal
395 resolution because it will have the slowest-to-reach detectable concentration. However, making
396 measurements in the dynamic range requires consistency of extraction times as differences in
397 time will lead to variations of extraction yields in a range that can be estimated from the SPME
398 extraction time profiles (**Fig 1D-E**). Given the dynamic nature of brain networks and the lack of
399 a stable equilibrium point, we expect consistency in brain states to be one of the biggest factors
400 in reducing replicated variability. Moreover, SPME measurements are inherently an average of
401 the temporal dynamics of the target tissue milieu. This means that due to the bi-directional
402 exchange of neuromodulators from the extracellular space and the SPME coating, longer periods
403 of stable concentration gradients will be more strongly reflected in the extracted measurements.

404 *Utility and Ease of Use.* SPME based microprobe extraction allows for multiple
405 simultaneous measurements that can be reliably repeated within the same measurement sessions
406 at the same locations with no evidence of damage induced disruption of the neurochemical
407 environment. Another critical advantage of SPME over comparable MS-analysis based methods
408 such as MD is its ease of use and accessibility. Due to their similar size to recording
409 microelectrodes used for electrophysiology, little adjustment is required for conducting SPME
410 measurements using existing acute microelectrode positioning systems. Measurements in deeper
411 structures should use an accompanying guide tube (**Fig 1C**) as travelling through non-target
412 tissue will result in unwanted chemical collection. Beyond the collection, a chemistry core could
413 apply LC-MS/MS to the probes allowing for relatively easy quantitation of extracellular
414 compounds of interest.

415 *Detection Methods.* SPME is ultimately a sampling method, much like MD, that provides
416 data for analytical tools such as chromatography and mass spectrometry. In fact, once SPME
417 analytes have been desorbed from the probe into a solvent, data provided by SPME and MD are
418 treated very much the same. Thus, the advancement in detection limits and reliability of post-hoc
419 analytical methods utilized by MD also benefit SPME, and vice versa. However, SPME sample
420 analysis is more reliably and conveniently coupled to LC-MS/MS as it lacks issues such as high
421 salt content of collected dialysate that MD suffers from (Guihen and Connor 2009).

422 *Extension of SPME measurements beyond classical neuromodulators*. A unique
423 advantage of SPME over alternative methods of in vivo detection of compounds within the brain
424 is its potential affinity for hydrophobic compounds. Although MD is capable of collecting
425 metabolomics data similarly to SPME (Anderzhanova and Wotjak 2013; Li et al. 2012; Zhang et
426 al. 2007b), the artificial cerebra-spinal fluid that is commonly traversing the semi-permeable

427 membrane better facilitates the collection of hydrophilic molecules. This means that molecules
428 that cross the semi-permeable membrane and are therefore collected and quantified through LC-
429 MS are much more likely to be hydrophilic. SPME, in contrast, provides balanced analyte
430 coverage, which means that in principle certain SPME matrix coatings have similar affinity for
431 both hydrophilic or hydrophobic compounds (Reyes-garcés et al. 2018). Data collected here
432 includes other neurochemicals of interest such as amino acids (e.g. glutamine, taurine,
433 phenylalanine, etc) that we reliably detected but do not discuss here. In practice, the detection of
434 very polar molecules such as monoamines and catecholamines requires coating chemistry that
435 facilitates hydrophilic compound extraction. Comparatively many lipids play important roles in
436 intracellular signaling and have been suggested to provide biomarkers for psychiatric disorders
437 (Tamiji and Crawford 2011; Yehuda et al. 1999), therefore making SPME a potentially versatile
438 and comprehensive tool for brain neurochemistry studies.
439
440 **Implications for Understanding and Treating Psychiatric Disease States.** Most psychiatric
441 disorders are accompanied by neuromodulatory dysregulation (Millan et al. 2012). However, this
442 fact is seldom studied in a multi-modulatory manner with a single or few nuclei or
443 neurochemicals being observed at a time. This is an increasingly evident problem because
444 models attributing symptoms of a disorder to a single neuromodulator often fall short in
445 explaining many symptoms (Bohnen et al. 2015; Remy et al. 2005). For example, in Parkinson's
446 disease, outside of the well characterized dopaminergic deficits, there is evidence for deficits in
447 noradrenergic, cholinergic and serotonergic systems as well (Halliday et al. 1990, 2014; Moehle
448 et al. 2017). Many cognitive deficits observed within Parkinson's disease are linked to such non-
449 dopaminergic deficits. Such findings emphasize the need to simultaneously observe multiple

450 neuromodulatory systems. Thus the simultaneous measurement of multiple neuromodulators, in
451 multiple brain regions within healthy and clinical populations will allow for a better
452 understanding of the underlying causes of symptoms and progression of psychiatric disorders
453 (Anderzhanova and Wotjak 2015; Avery and Krichmar 2017; Millan et al. 2012).

454 A better understanding of psychiatric disorders through multi-modulator methods may
455 also lead to more accurate understanding of the action of pharmacological agents. Previously,
456 many studies aimed at identifying the locus of action of a pharmacological agent have used local
457 injection methods such as iontophoresis or microinjections (Lapiz and Morilak 2006; Wang et al.
458 2007). Although highly informative about the role of neuromodulators in modulating the activity
459 of individual cells and circuits, this approach does not allow physiologically realistic exploration
460 of a systemically administered pharmacological agent. Pharmacological agents are often
461 administered in some systemic fashion and even with highly specific receptor affinities, may
462 interact with multiple neuromodulatory systems through the actions of heteroreceptors (Avery
463 and Krichmar 2017; Gobert et al. 1998; Millan et al. 2015). Multi-modulator measurements, as
464 described here, will allow for a better understanding of pharmacological agents, as well as
465 provide novel insights into the development of more effective drugs or combinations of drugs to
466 better treat the clinical population.

467

468 **Conclusion**. We described a novel SPME protocol capable of simultaneous, multi-modulator
469 measurements of multiple brain regions. Our results suggest that SPME both supplements
470 current methods of neuromodulator detection and allows for novel measurements previously not
471 possible for the investigation and dissection of neuromodulatory systems, their role in
472 physiological brain processes and their modulation by pharmacological agents.

Acknowledgments

This research was supported by grants from the Canadian Institutes of Health Research (CIHR), the Natural Sciences and Engineering Research Council of Canada (NSERC) and the Ontario Ministry of Economic Development and Innovation (MEDI). We thank Dr. Hongying Wang for invaluable help with animal care. We thank Thermo Scientifc for providing the triple quadrupole mass spectrometer TSQ Quantiva used in this work as a loan to our laboratory. The authors thankfully acknowledge Pfizer Canada Inc., Merck Canada Inc., Quebec Consortium for Drug Discovery (CQDM), Brain Canada, and Ontario Brain Institute for the grant "Solid phase microextraction-based integrated platform for untargeted and targeted in vivo brain studies".

Conflicts of interest

None of the authors have any conflict to disclose.

485 **References**
486
487 **Alam N**, **Pawliszyn J**. Numerical Simulation and Experimental Validation of Calibrant-Loaded
488 Extraction Phase Standardization Approach. *Anal Chem* 88: 8632–8639, 2016.
489 **Anderzhanova E**, **Wotjak CT**. Brain microdialysis and its applications in experimental
490 neurochemistry. *Cell Tissue Res* 354: 27–39, 2013.
491 **Anderzhanova E**, **Wotjak CT**. NextGen Brain Microdialysis : Applying Modern Metabolomics
492 Technology to the Analysis of Extracellular Fluid in the Central Nervous System. *Mol*
493 *Neuropsychiatry* 1: 60–67, 2015.
494 **Arnsten AFT**, **Paspalas CD**, **Gamo NJ**, **Yang Y**, **Wang M**. Dynamic network connectivity: A
495 new form of neuroplasticity. *Trends Cogn Sci* 14: 365–375, 2010.
496 **Ascenzo MD**, **Fellin T**, **Terunuma M**, **Revilla-sanchez R**, **Meaney DF**, **Auberson YP**, **Moss**
497 **SJ**, **Haydon PG**. mGluR5 stimulates gliotransmission in the nucleus accumbens. *Proc Natl Acad*
498 *Sci* 104: 1995–2000, 2006.
499 **Avery MC**, **Krichmar JL**. Neuromodulatory Systems and Their Interactions : A Review of
500 Models , Theories , and Experiments. *Front Neural Circuits* 11: 1–18, 2017.
501 **Bohnen NB**, **Albin R**, **Muller MLTM**, **Petrou M**, **Kotagal V**, **Koeppe RA**, **Scott PJH**, **Frey**
502 **KA**. Frequency of Cholinergic and Caudate Nucleus Dopaminergic Deficits Across the
503 Predemented Cognitive Spectrum of Parkinson Disease and Evidence of Interaction Effects.
504 *JAMA Neurol* 72: 194–200, 2015.
505 **Cudjoe E**, **Bojko B**, **de Lannoy I**, **Saldivia V**, **Pawliszyn J**. Solid-Phase Microextraction: A
506 Complementary In Vivo Sampling Method to Microdialysis. *Angew Chemie Int Ed* 52: 12124–
507 12126, 2013.
508 **Cudjoe E**, **Pawliszyn J**. Optimization of solid phase microextraction coatings for liquid
509 chromatography mass spectrometry determination of neurotransmitters. *J Chromatogr A* 1341:
510 1–7, 2014.
511 **Dale N**, **Hatz S**, **Tian F**, **Llaudet E**. Listening to the brain: Microelectrode biosensors for
512 neurochemicals. *Trends Biotechnol* 23: 420–428, 2005.
513 **Deng J**, **Yang Y**, **Wang X**, **Luan T**. Strategies for coupling solid-phase microextraction with
514 mass spectrometry. *TrAC - Trends Anal Chem* 55: 55–67, 2014.
515 **Fisher RE**, **Morris ED**, **Alpert NM**, **Fischman AJ**. In Vivo Imaging of Neuromodulatory
516 Synaptic Transmission Using PET : A Review of Relevant Neurophysiology. *Hum Brain Mapp*
517 3: 24–34, 1995.
518 **Ghersi C**, **Bonfanti A**, **Manzari B**, **Feligioni M**, **Raiteri M**, **Pittaluga A**. Pharmacological
519 heterogeneity of release-regulating presynaptic AMPA / kainate receptors in the rat brain : study
520 with receptor antagonists. *Neurochem Int* 42: 283–292, 2003.
521 **Gobert A**, **Audinot V**, **Cistarelli L**, **Millan MJ**. Simultaneous quantification of serotonin,
522 dopamine and noradrenaline levels in single frontal cortex dialysates of freely-moving rats
523 reaveals a complex pattern of reciprocal auto- and heteroreceptor-mediated control of release.
524 *Neuroscience* 84: 413–429, 1998.
525 **Goldman-Rakic PS**, **Lidow MS**, **Gallager DW**. Overlap of dopaminergic, adrenergic, and
526 serotoninergic receptors and complementarity of their subtypes in primate prefrontal cortex. *J*
527 *Neurosci* 10: 2125–2138, 1990.
528 **Gómez-Ríos GA**, **Tascon M**, **Reyes-garcés N**, **Boyacı E**. Quantitative analysis of biofluid spots
529 by coated blade spray mass spectrometry , a new approach to rapid screening. *Sci Rep* 7: 1–7,
530 2017.

Granger AJ, **Mulder N**, **Saunders A**, **Sabatini BL**. Cotransmission of acetylcholine and GABA. *Neuropharmacology* 100: 40–46, 2016.
Grilli M, **Zappettini S**, **Zanardi A**, **Lagomarsino F**, **Pittaluga A**, **Zoli M**, **Marchi M**. Exposure to an enriched environment selectively increases the functional response of the pre-synaptic NMDA receptors which modulate noradrenaline release in mouse hippocampus. *J Neurochem* 110: 1598–1606, 2009.
Guihen E, **Connor WTO**. Current separation and detection methods in microdialysis the drive towards sensitivity and speed. *Electrophoresis* 30: 2062–2075, 2009.
Haber SN, **Knutson B**. The reward circuit: Linking primate anatomy and human imaging. *Neuropsychopharmacology* 35: 4–26, 2010.
Halliday GM, **Leverenz JB**, **Schneider JS**, **Adler CH**. The Neurobiological Basis of Cognitive Impairment in Parkinson's Disease. *Mov Disord* 29: 634–650, 2014.
Halliday GM, **Li YW**, **Blumbergs PC**, **Joh TH**, **Cotton PRGH**, **Howe PRC**, **Blessing WW**, **Geffen LB**. Neuropathology of Immunohstochemically Idendied Brainstem Neurons in Parkinson's Disease. *Am Neurol Assoc* 27: 373–385, 1990.
Hassan SF, **Zumut S**, **Burke PG**, **Mcmullan S**, **Cornish JL**, **Goodchild AK**. Comparison of noradrenlaine, dopamine and serotonin in mediating the tachycardic and thermogenic effects of methamphetamine in the ventral medial prefrontal cortex. *Neuroscience* 295: 209–220, 2015.
Hassani SA, **Oemisch M**, **Balcarras M**, **Westendorff S**, **Ardid S**, **van der Meer MA**, **Tiesinga P**, **Womelsdorf T**. A computational psychiatry approach identifies how alpha-2A noradrenergic agonist Guanfacine affects feature-based reinforcement learning in the macaque. *Sci Rep* 7: 40606, 2017.
Howe WM, **Gritton HJ**, **Lusk NA**, **Roberts EA**, **Hetrick VL**, **Berke JD**, **Sarter M**. Acetylcholine Release in Prefrontal Cortex Promotes Gamma Oscillations and Theta–Gamma Coupling during Cue Detection. *J Neurosci* 37: 3215–3230, 2017.
Jacobs CB, **Peairs MJ**, **Venton BJ**. Review: Carbon nanotube based electrochemical sensors for biomolecules. *Anal Chim Acta* 662: 105–127, 2010.
Kennedy RT. Emerging trends in in vivo neurochemical monitoring by microdialysis. *Curr Opin Chem Biol* 17: 860–867, 2013.
Kodama T, **Hikosaka K**, **Honda Y**, **Kojima T**, **Tsutsui K**, **Watanabe M**. Dopamine and glutamate release in the anterior default system during rest : A monkey microdialysis study. *Behav Brain Res* 294: 194–197, 2015.
Kodama T, **Hikosaka K**, **Watanabe M**. Differential changes in glutamate concentration in the primate prefrontal cortex during spatial delayed alternation and sensory-guided tasks. *Exp Brain Res* 145: 133–141, 2002.
Kodama T, **Kojima T**, **Honda Y**, **Hosokawa T**, **Tsutsui K**, **Watanabe M**. Oral Administration of Methylphenidate (Ritalin) Affects Dopamine Release Differentially Between the Prefrontal Cortex and Striatum: A Microdialysis Study in the Monkey. *J Neurosci* 37: 2387–2394, 2017.
Kreitzer AC. Physiology and pharmacology of striatal neurons. *Annu Rev Neurosci* 32: 127–47, 2009.
Lapiz MDS, **Morilak DA**. Noradrenergic modulation of cognitive function in rat medial prefrontal cortex as measured by attentional set shifting capability. *Neuroscience* 137: 1039–1049, 2006.
Li J, **von Pföstl V**, **Zaldivar D**, **Zhang X**, **Logothetis NK**, **Rauch A**. Measuring multiple neurochemicals and related metabolites in blood and brain of the rhesus monkey by using dual microdialysis sampling and capillary hydrophilic interaction chromatography-mass spectrometry.

Anal Bioanal Chem 402: 2545–2554, 2012.
Luccini E, **Musante V**, **Neri E**, **Brambilla Bas M**, **Severi P**, **Raiteri M**, **Pittaluga A**. Functional interactions between presynaptic NMDA receptors and metabotropic glutamate receptors co-expressed on rat and human noradrenergic terminals. *Br J Pharmacol* 151: 1087–1094, 2007.
Marder E. Overview Neuromodulation of Neuronal Circuits: Back to the Future. *Neuron* 76: 1–11, 2012.
Marder E, **O'Leary T**, **Shruti S**. Neuromodulation of Circuits with Variable Parameters: Single Neurons and Small Circuits Reveal Principles of State-Dependent and Robust Neuromodulation. *Annu Rev Neurosci* 37: 329–346, 2014.
McGinley MJ, **Vinck M**, **Reimer J**, **Batista-Brito R**, **Zagha E**, **Cadwell CR**, **Tolias AS**, **Cardin JA**, **McCormick DA**. Waking State: Rapid Variations Modulate Neural and Behavioral Responses. *Neuron* 87: 1143–1161, 2015.
Millan MJ, **Agid Y**, **Brüne M**, **Bullmore ET**, **Carter CS**, **Clayton NS**, **Connor R**, **Davis S**, **Deakin B**, **DeRubeis RJ**, **Dubois B**, **Geyer MA**, **Goodwin GM**, **Gorwood P**, **Jay TM**, **Joëls M**, **Mansuy IM**, **Meyer-Lindenberg A**, **Murphy D**, **Rolls E**, **Saletu B**, **Spedding M**, **Sweeney J**, **Whittington M**, **Young LJ**. Cognitive dysfunction in psychiatric disorders: characteristics, causes and the quest for improved therapy. *Nat Rev Drug Discov* 11: 141–168, 2012.
Millan MJ, **Goodwin GM**, **Meyer-lindenberg A**, **Ove S**. Learning from the past and looking to the future : Emerging perspectives for improving the treatment of psychiatric disorders. *Eur Neuropsychopharmacol* 25: 599–656, 2015.
Moehle MS, **Pancani T**, **Byun N**, **Yohn SE**, **Wilson GH**, **Dickerson JW**, **Remke DH**, **Xiang Z**, **Niswender CM**, **Wess J**, **Jones CK**, **Lindsley CW**, **Rook JM**, **Conn PJ**. Cholinergic Projections to the Substantia Nigra Pars Reticulata Inhibit Dopamine Modulation of Basal Ganglia through the M4Muscarinic Receptor. *Neuron* 96: 1358–1372, 2017.
Moghaddam B. Stress Preferentially Increases Extraneurona Levels of Excitatory Amino Acids in the Prefrontal Cortex : Comparison to Hippocampus and Basal Ganglia. *J Neurochem* 60: 1650–1657, 1993.
Moussawi K, **Riegel A**, **Nair S**, **Kalivas PW**, **Bargas J**, **Nacional U**. Extracellular glutamate : functional compartments operate in different concentration ranges. *Front Syst Neurosci* 5: 1–9, 2011.
Oemisch M, **Westendorff S**, **Oemisch M**, **Westendorff S**, **Everling S**, **Womelsdorf XT**. Interareal Spike-Train Correlations of Anterior Cingulate and Dorsal Prefrontal Cortex during Attention Shifts Interareal Spike-Train Correlations of Anterior Cingulate and Dorsal Prefrontal Cortex during Attention Shifts. *J Neurosci* 35: 13076–13089, 2015.
Parikh V, **Kozak R**, **Martinez V**, **Sarter M**. Prefrontal Acetylcholine Release Controls Cue Detection on Multiple Timescales. *Neuron* 56: 141–154, 2007.
Pawliszyn J. Theory of Solid-Phase Microextraction. In: *Handbook of Solid Phase Microextraction*, edited by Pawliszyn J. Elsevier, 2012, p. 13–59.
Paxinos G, **Huang X**, **Toga A**. *The Rhesus Monkey Brain in Stereotaxic Coordinates*. 2000.
Pittaluga A. Presynaptic release-regulating mGlu1 receptors in central nervous system. *Front Pharmacol* 7: 1–15, 2016.
Pittaluga A, **Feligioni M**, **Longordo F**, **Luccini E**, **Raiteri M**. Trafficking of presynaptic AMPA receptors mediating neurotransmitter release : Neuronal selectivity and relationships with sensitivity to cyclothiazide. *Neuropharmacology* 50: 286–296, 2006.
Reimer J, **Froudarakis E**, **Cadwell CR**, **Yatsenko D**, **Denfield GH**, **Tolias AS**. Pupil

623 Fluctuations Track Fast Switching of Cortical States during Quiet Wakefulness. *Neuron* 84: 355–
624 362, 2014.
625 **Reimer J**, **McGinley MJ**, **Liu Y**, **Rodenkirch C**, **Wang Q**, **McCormick DA**, **Tolias AS**. Pupil
626 fluctuations track rapid changes in adrenergic and cholinergic activity in cortex. *Nat Commun* 7:
627 1–7, 2016.
628 **Remy P**, **Doder M**, **Lees A**, **Turjanski N**, **Brooks D**. Depression in Parkinson ' s disease: loss
629 of dopamine and noradrenaline innervation in the limbic system. *Brain* 128: 1314–1322, 2005.
630 **Reyes-garcés N**, **Gionfriddo E**, **Gómez-Ríos GA**, **Alam MN**, **Boyaci E**, **Bojko B**, **Singh V**,
631 **Grandy J**, **Pawliszyn J**. Advances in Solid Phase Microextraction and Perspective on Future
632 Directions. *Anal Chem* 90: 302–360, 2018.
633 **Santana N**, **Mengod G**, **Artigas F**. Expression of a1-adrenergic receptors in rat prefrontal
634 cortex: cellular co-localization with 5-HT2A receptors. *Int J Neuropsychopharmacol* 16: 1139–
635 1151, 2018.
636 **Santello M**, **Calì C**, **Bezzi P**. Gliotransmission and the Tripartite Synapse. In: *Synaptic*
637 *Plasticity. Advances in Experimental Medicine and Biology*, edited by Kreutz M, Sala C. 2012,
638 p. 307–331.
639 **Schwartz J**, **Javitch J**. Neurotransmitters. In: *Principles of Neural Science*, edited by Kandel E,
640 Schwartz J, Jessell T, Siegelbaum S, Hudspeth A. 2013, p. 289–306.
641 **Syková E**. Extrasynaptic volume transmission and diffusion parameters of the extracellular
642 space. *Neuroscience* 129: 861–876, 2004.
643 **Tamiji J**, **Crawford A**. The Neurobiology of Lipid Metabolism in. *Eur PMC* 18: 98–112, 2011.
644 **Thiele A**, **Bellgrove MA**. Neuromodulation of Attention. *Neuron* 97: 769–785, 2018.
645 **Vartak D**, **Togt C Van Der**, **Vugt B Van**, **Roelfsema PR**. Electrochemical measurement of
646 acetylcholine in the dorsolateral prefrontal cortex : A technical report. *BioRXiv* 1–25, 2017.
647 **Vizi ES**. Role of high-affinity receptors and membrane transporters in nonsynaptic
648 communication and drug action in the central nervous system. *Pharmacol Rev* 52: 63–89, 2000.
649 **Wang JKT**, **Andrews H**, **Thukral V**. Presynaptic Glutamate Receptors Regulate Noradrenaline
650 Release from Isolated Nerve Terminals. *J Neurochem* 58: 204–211, 1992.
651 **Wang M**, **Ramos BP**, **Paspalas CD**, **Shu Y**, **Simen A**, **Duque A**, **Vijayraghavan S**, **Brennan**
652 **A**, **Dudley A**, **Nou E**, **Mazer J a.**, **McCormick D a.**, **Arnsten a. FT**. alpha2A-Adrenoceptors
653 Strengthen Working Memory Networks by Inhibiting cAMP-HCN Channel Signaling in
654 Prefrontal Cortex. *Cell* 129: 397–410, 2007.
655 **Watanabe M**, **Kodama T**, **Hikosaka K**. Increase of Extracellular Dopamine in Primate
656 Prefrontal Cortex During a Working Memory Task. *J Neurophysiol* 78: 2795–2798, 1997.
657 **Watson CJ**, **Venton BJ**, **Kennedy RT**. In Vivo Measurements of Neurotransmitters by
658 Microdialysis Sampling. *Anal Chem* 78: 1391–1399, 2006.
659 **Yehuda S**, **Rabinovitz S**, **Mostofsky DI**. Mini-Review Essential Fatty Acids Are Mediators of
660 Brain Biochemistry and Cognitive Functions. *J Neurosci Res* 56: 565–570, 1999.
661 **Zapata A**, **Chefer VI**, **Parrot S**, **Denoroy L**. Detection and Quantification of Neurotransmitters
662 in Dialysates. *Curr Protoc Neurosci* 63: 1–35, 2013.
663 **Zhang X**, **Es-haghi A**, **Musteata FM**, **Ouyang G**, **Pawliszyn J**. Quantitative in Vivo
664 Microsampling for Pharmacokinetic Studies Based on an Integrated Solid-Phase Microextraction
665 System. *Anal Chem* 79: 4507–4513, 2007a.
666 **Zhang X**, **Rauch A**, **Lee H**, **Xiao H**, **Rainer G**, **Logothetis N**. Capillary hydrophilic interaction
667 chromatography/mass spectrometry for simultaneous determination of multiple neurotransmitters
668 in primate cerebral cortex. *Rapid Commun Mass Spectrom* 21: 3621–3628, 2007b.

669 **Fig 1. SPME sampling procedure, extraction time profiles and measurement locations**.
670 (A) Dimensions of the SPME probe and the accompanying cannula. There was a 3000 µm buffer
671 from the opening of the cannula and the start of the SPME coating. The SPME coating was 195
672 µm at the tip. The SPME coating made up the terminal 3000 µm of the entire probe and was
673 placed in a cannula with an internal diameter of 200 µm and an external diameter of 270 µm. **(**B)
674 Tungsten microelectrodes were lowered into the brain guided by 3 T magnetic resonance (MR)
675 images in order to map the depth at which detectable spiking was observed matching
676 expectations from the MR images. (C) SPME probes and their accompanying cannulas in all
677 brain areas were then simultaneously lowered to 200 µm above the point of first observable
678 firing in the target brain region and the SPME probes were lowered to expose only the 3000 µm
679 SPME coating. After 20 minutes of extraction, the SPME probes were then retracted 3000 µm
680 back into the cannula and the probes plus their accompanying cannulas were removed from the
681 brain. The table inset into the figure provides the velocities and times of each probe and cannula
682 as they transitioned between the extraction steps. (D) Extraction quantities of Glutamate in ng
683 and (E) Dopamine in ng over time. The linear "kinetic" regime and "equilibrium" regime are
684 labelled with the dynamic range being in between. (F**)** Anatomical locations of SPME sampling
685 events in the right hemisphere of two Rhesus Macaques. Target brain regions are highlighted in
686 red and include two cortical regions, prefrontal cortex (PFC) area 8 and premotor cortex (PreM)
687 area 6 as well as a subcortical region: the head of the caudate.
688
689 **Fig 2. Changes in SPME sampling over time.**
690 Changes in the normalized concentrations of the observed neuromodulators across daily
691 sampling sessions in each sampled brain region. The median concentration of (A) Glutamate (B)
692 acetylcholine (C) choline and dopamine (D) with standard error of the median plotted for each
693 sampling time and location. Data was normalization for each subject separately and for the
694 respective neurochemical and area combinations. Sampling locations are represented by different
695 lines: solid line for the prefrontal cortex, dashed line for the premotor cortex and dotted line for
696 the caudate nucleus. Sampling events were 20 minutes in length and the time between the end of
697 one sampling event to the start of the next sampling event was 40 minutes (STD 2 minutes)
698 making the second sampling event 40 minutes and the third 100 minutes from the initial
699 measurement. No significant change was observed for any neuromodulator in any brain region
700 (Wisconsin rank sum test). Note that a single prefrontal choline data point was excluded in this
701 analysis for being >4 standard deviations from the median (data point is present in **Fig 3a**).
702
703 **Fig 3. SPME sampling of the macaque brain.**
704 SPME probes extract from the cortex (PFC and PreM6) as well as the caudate of two adult
705 macaques after 20 minutes of extraction within the respective brain region. Median and standard
706 error of the median of n= 12 probes for animal As and n= 9 probes for animal Ke with no data
707 excluded. Four neuromodulators were reliably measured: glutamate, dopamine, acetylcholine,
708 and choline (orange, green, purple, red respectively). All brain regions had high concentrations
709 of glutamate and relatively much lower concentrations of acetylcholine and choline extracted
710 (with the exception of animal Ke PreM6 lacking detectable acetylcholine). The only tested
711 region to yield measurable dopamine was the caudate. The dashed blue line depicts the limit of
712 detection (LOD).
713
714

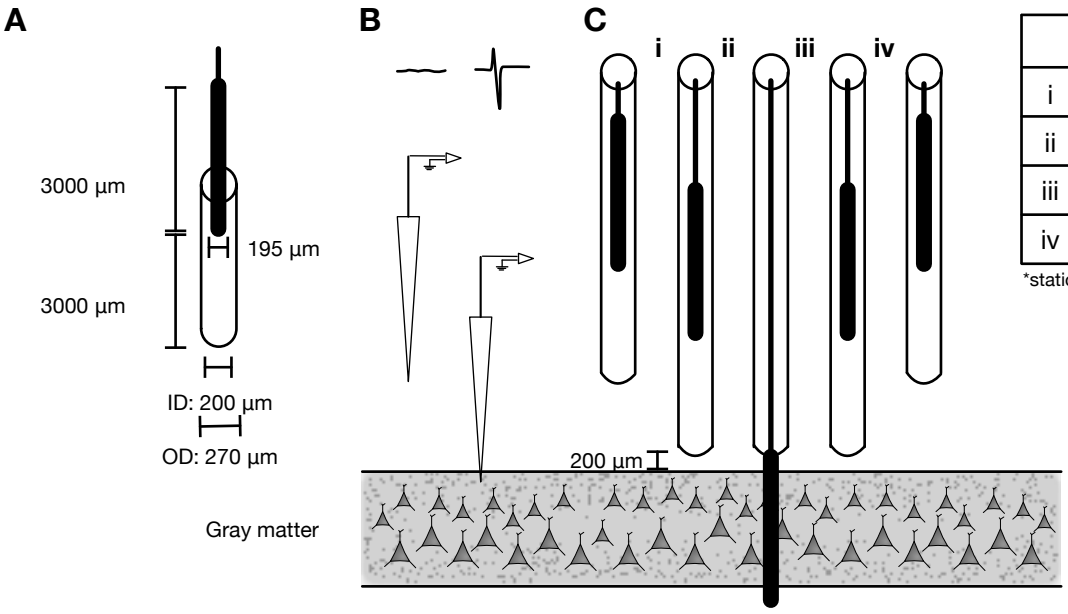

	fibre	cannula	time
i	30 µm/s	30 µm/s	variable
ii	30 µm/s	-	200s
iii	30 µm/s	-	1200s* + 200s
iv	30 µm/s	30 µm/s	variable

*stationary: extraction period of 20 min

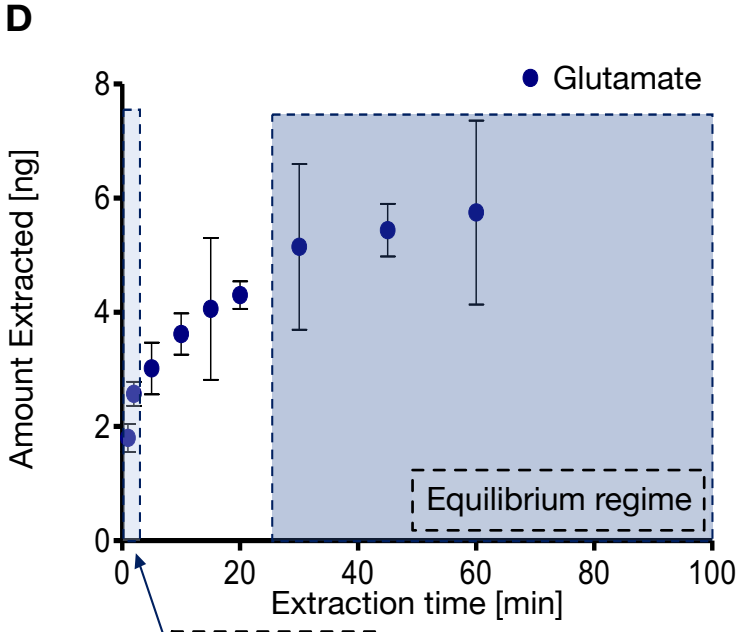

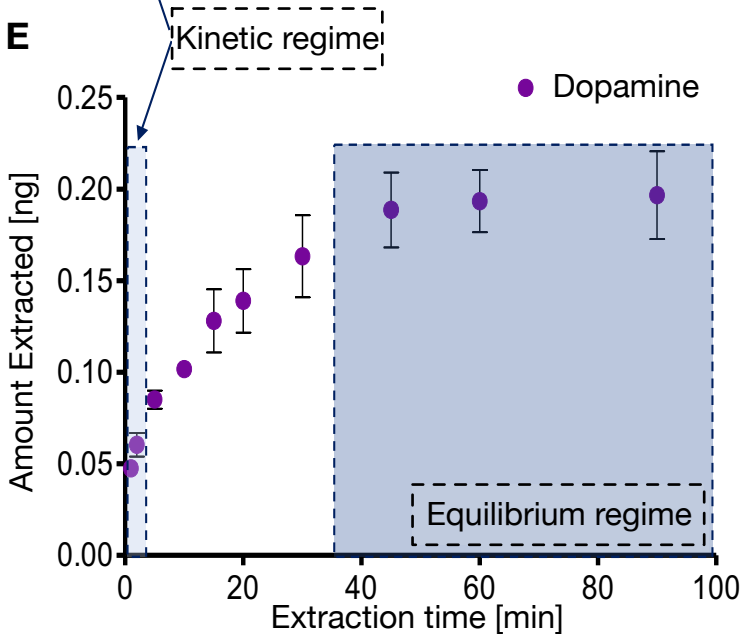

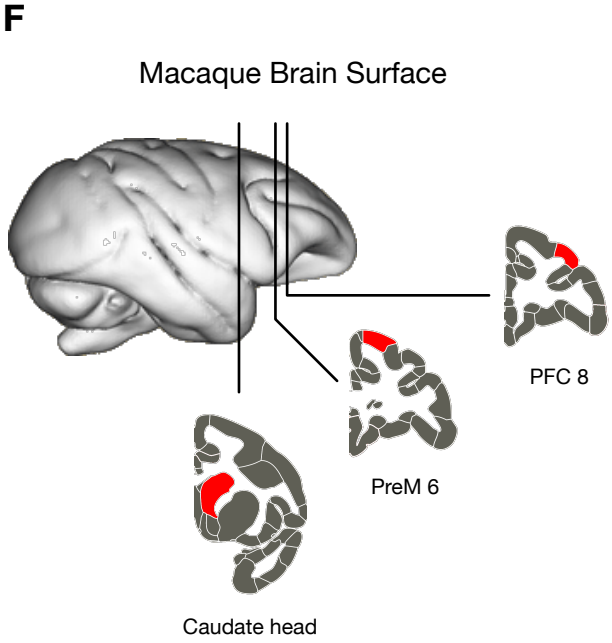

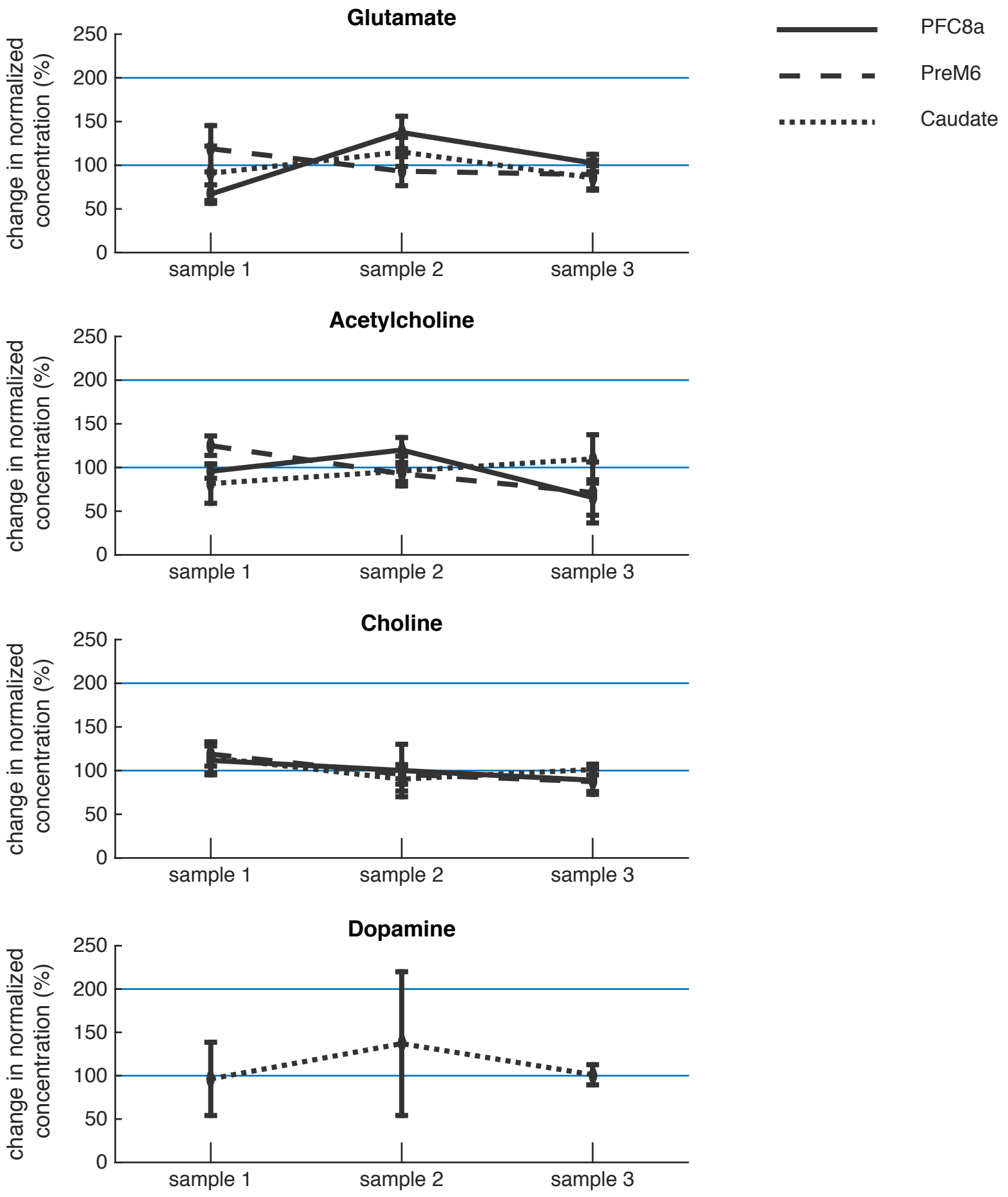
Glutamate
Acetylcholine
Choline
Dopamine
change in normalized concentration (%)
250
200
150
100
50
0
sample 1
sample 2
sample 3
PFC8a
PreM6
Caudate

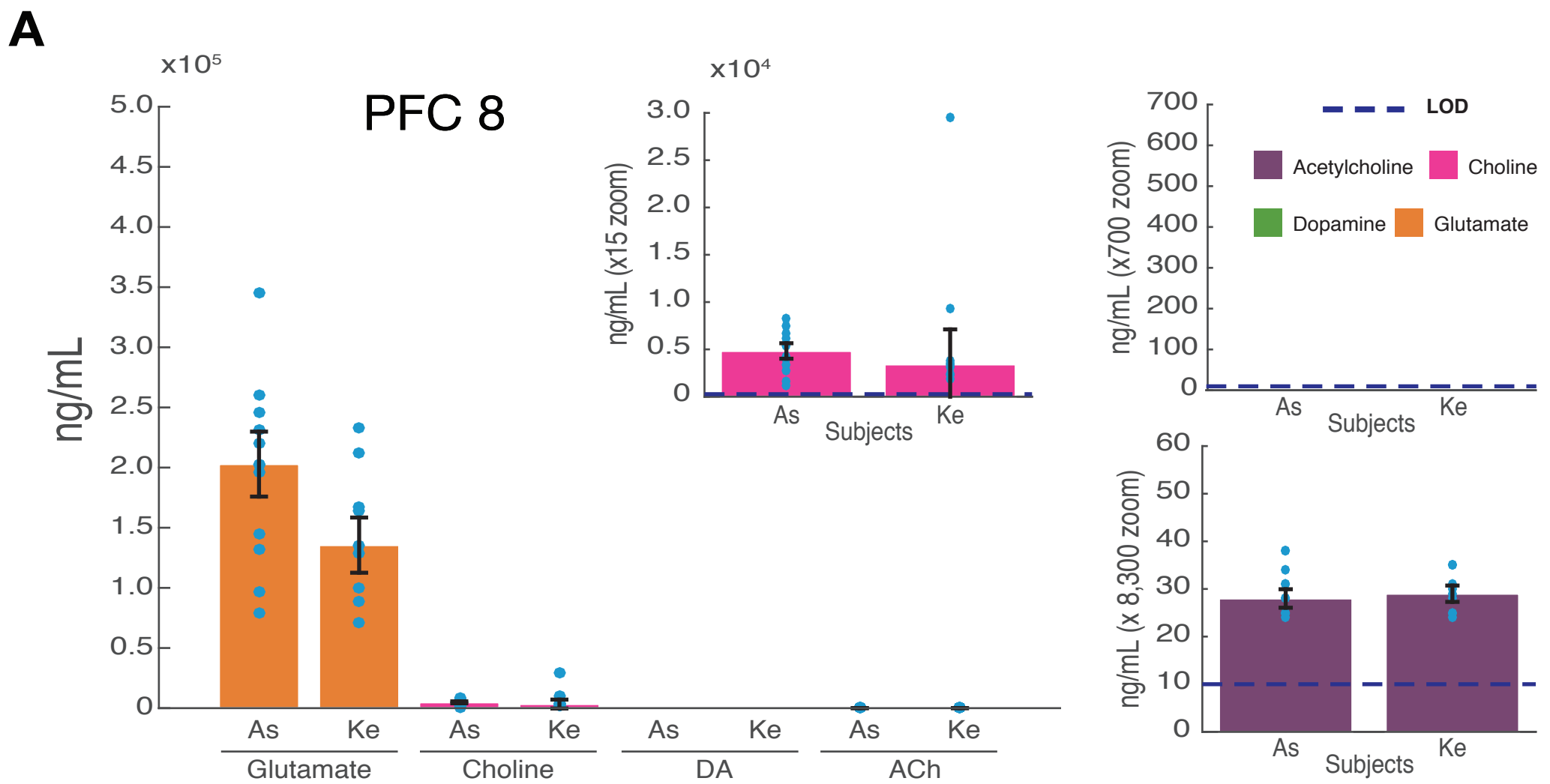
A
PFC 8
x10⁵
ng/mL
5.0
4.5
4.0
3.5
3.0
2.5
2.0
1.5
1.0
0.5
0
As
Ke
Glutamate
Choline
DA
ACh
x10⁴
ng/mL (x15 zoom)
Subjects
LOD
Acetylcholine
Choline
Dopamine
Glutamate
ng/mL (x700 zoom)
ng/mL (x 8,300 zoom)

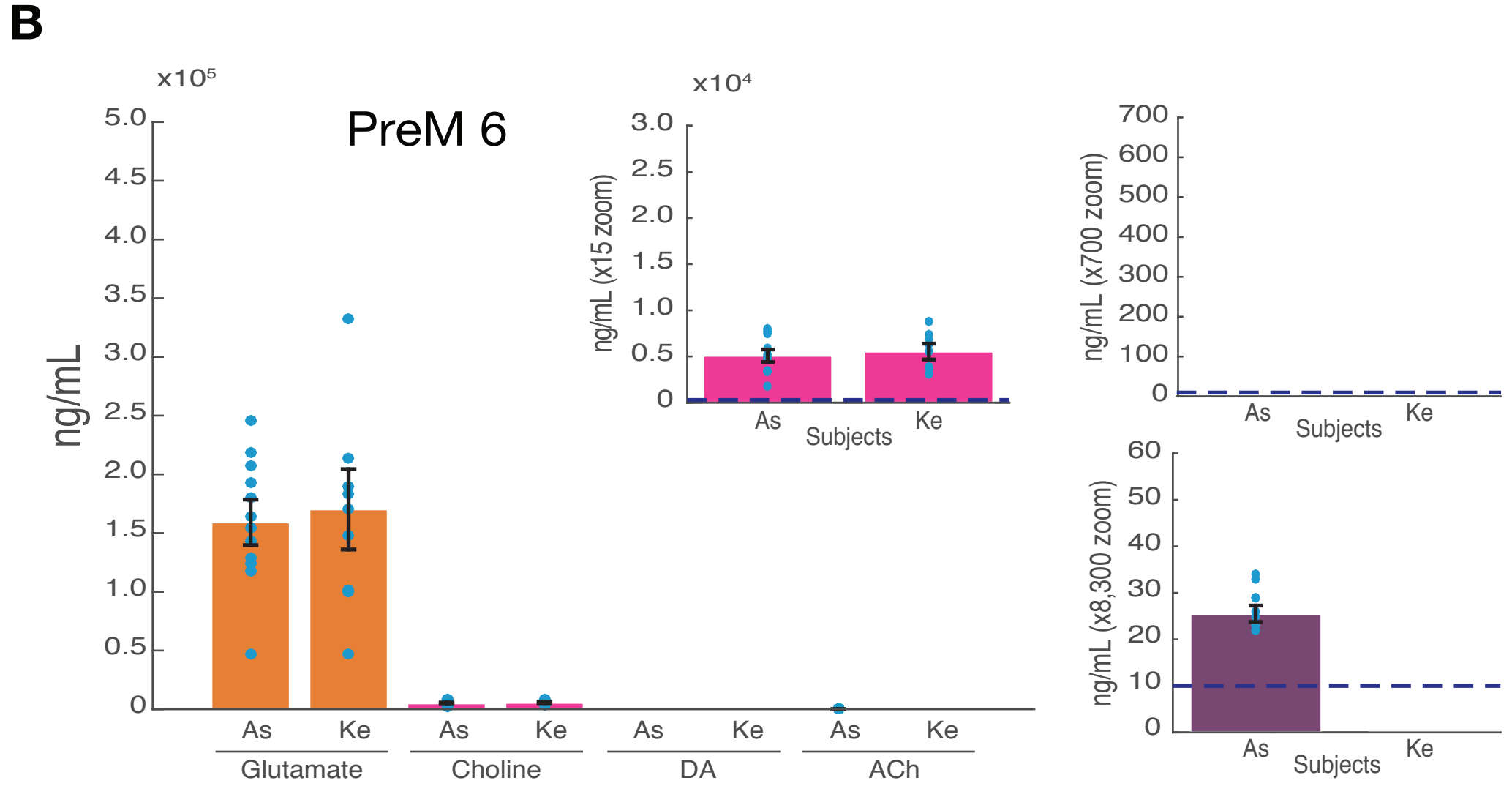
B
PreM 6
x10⁵
ng/mL
5.0
4.5
4.0
3.5
3.0
2.5
2.0
1.5
1.0
0.5
0
As
Ke
Glutamate
Choline
DA
ACh
x10⁴
ng/mL (x15 zoom)
Subjects
ng/mL (x700 zoom)
ng/mL (x8,300 zoom)

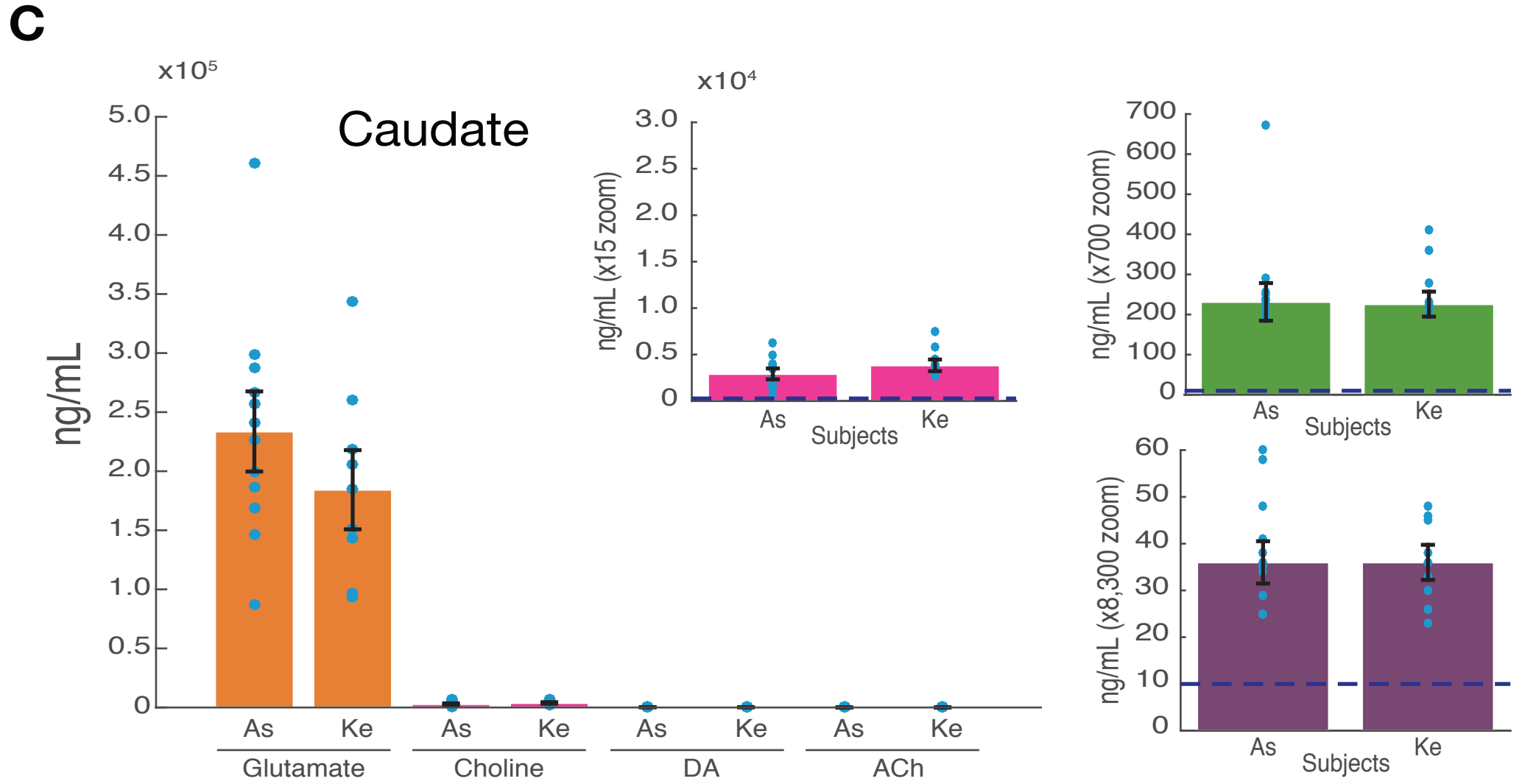
C
Caudate
x10⁵
ng/mL
5.0
4.5
4.0
3.5
3.0
2.5
2.0
1.5
1.0
0.5
0
As
Ke
Glutamate
Choline
DA
ACh
x10⁴
ng/mL (x15 zoom)
Subjects
ng/mL (x700 zoom)
ng/mL (x8,300 zoom)

Supplementary Methods

Chemicals, Reagents and Materials

The LC-MS-grade solvents methanol (MeOH), acetonitrile (ACN), isopropanol (IPA) and water, as well as the acetylcholinesterase inhibitor phenylmethylsulfonyl fluoride (PMSF) were purchased from Fisher Scientifc. Formic acid, polyacrylonitrile (PAN), N,N-dimethylformamide (DMF) and the standards of neurotransmitters: γ-aminobutyric acid (GABA), glutamic acid (Glu), acetylcholine (ACh), histamine (Hist), serotonin (5-HT), dopamine (DA) and choline (Cho) as well as their deuterated analogues were purchased from Millipore Sigma (Oakville, ON, Canada). Epinephrine (Epi), norepinephrine (NE) and their deuterated analogues were obtained from Cerilliant Corporation (Round Rock, TX, USA). Choline-D9, was purchased from Cambridge Isotope Laboratories (Tewksbury, MA, USA). The reagents used for synthesis of hydrophilic-lipophilic balance polymer particles functionalized with strong cation exchange groups, as well as compounds for preparation of PBS were purchased from Millipore-Sigma. The stainless steel wire (stainless steel grade AISI 304, 150 µm diameter) used for manufacturing of SPME probes was purchased from Unimed S.A. (Lausanne, Switzerland). The stainless steel tubing used as guiding cannulas (270 µm O.D.; 200±5 µm I.D.) was obtained from Vita Needle (Needham, MA, USA).

LC-MS/MS Analysis

On the day of analysis, the SPME probes were defrosted and desorbed into 40 µL of water/ACN/MeOH 40:30:30 (v/v/v) mixture containing 1 % of formic acid and a mixture of deuterated isotopologues of targeted neuromodulators (used as internal standards, IS) at 20 ng/mL. The desorption was carried out for 1 h with agitation at 1500 rpm. The extracts were injected into the LC-MS system for targeted neurotransmitter analysis within a few hours after desorption. All experiments were carried out using an Ultimate 3000RS HPLC system coupled to TSQ Quantiva triple quadrupole mass spectrometer (Thermo Fisher Scientific, San Jose, California, USA). Data processing was performed using Thermo software Xcalibur 4.0 and Trace Finder 4.1. For chromatographic separation of the target compounds, a modified method of what is previously reported (Cudjoe and Pawliszyn 2014) was used, adjusted to include more

targeted neuromodulators and their corresponding IS. A Kinetex® PFP LC column (100 x 2.1 mm, 1.7 µm; Phenomenex, Torrance, CA, USA) was held at 30°C with the mobile phase flow rate at 400 µL/min. The mobile phase A consisted of water/MeOH/ACN 90:5:5 (v/v/v) with 0.1 % formic acid, and mobile phase B was ACN/water 90:10 (v/v) with 0.1% of formic acid. The chromatographic gradient was applied starting from 100% B for 1 min and increasing the aqueous mobile phase A to 100% for 3 min with convex gradient function, held for 0.5 min and subsequent linear return to initial conditions and re-equilibration for 1 min, yielding total time of 6.5 min. The injection volume was 10 µL. MS/MS analysis was performed with electrospray ionization in positive mode under selected reaction monitoring conditions, with two MS/MS transitions for each neuromodulator (quantifier and qualifier) and one for each IS.

Quantitation of neuromodulators

Individual stock standard solutions of all targeted neuromodulators were prepared in methanol or water with 0.1% formic acid at a concentration of 1 mg/mL and stored at −80 °C for maximum of one month. In order to calculate the amounts of neuromodulators extracted by each probe, calibrator standards prepared in the same desorption solvent as real samples were analyzed in the same batch. This instrumental calibration curve was prepared in the range of 0.1-200 ng/mL by a serial dilution of the stock standard mixture of all compounds at 1µg/mL. The IS concentration was kept constant at 20 ng/mL in all calibrators, identically as in the real samples. The amounts extracted were calculated based on linear regression equation obtained from the analytical signal (the ratio of chromatographic peak areas of analytes and their corresponding IS) plotted against the concentration.

In order to calculate the concentrations of neuromodulators in brain, matrix-matched external calibration approach was used. The surrogate matrix consisted of 2% agar gel mixed with brain homogenate in the ratio 1:1 (*v/w)*. The homogenized brain tissue was earlier incubated with 1 mM PMSF for 1 h at 37°C to prevent enzymatic digestion of acetylcholine in the calibrator samples. Due to several target compounds being present in brain homogenate at high concentrations (e.g. for glutamate and choline the “blank” brain homogenate matrix doesn’t exist), their quantitation was based on signals of their deuterated isotopologues. The calibrator samples were prepared in the surrogate matrix with concentrations of neuromodulators ranging

from 5 to 3000 µg/mL for the isotopically labelled compounds or from 10 to 2000 ng/mL for the remaining compounds.

The extractions were carried out with SPME probes manufactured and pre-treated identically to the probes used for *in vivo* sampling and using the same 20 min extraction time and desorption conditions as for the real samples. The amounts of neuromodulators extracted from the calibrator samples were determined in the same way as described above and plotted against concentrations of calibrators. The resulting weighted linear regression equations were applied to the amounts of neuromodulators extracted from the *in vivo* samples, yielding values of concentrations of the compounds of interest in brain.

The limits of detection (LOD) were estimated as the levels corresponding to the signal to noise ratio of 3 and were calculated based on the signal of blank calibrator sample (considered as the noise).

Supplementary Results

Observed serotonin concentrations. Overall, serotonin concentrations were not observed as reliably as the other reported neurochemicals and therefore were excluded from the main analyses. However, in one of the animals, serotonin was observed near the LOD in the prefrontal cortex as well as the caudate in a subset of probes. Within the 9 probes placed in both areas, serotonin was detected in 22% of samples (2/9 probes) in the prefrontal cortex and 33% of samples (3/9 probes) in the caudate nucleus. Serotonin observations ranged from 149 ng/mL to 232 ng/mL with a median of 171 ng/mL (±18.5 ng/mL; standard error of the median) with a LOD of 100 ng/mL. The proximity of the measurements to the LOD suggest that the other probes likely collected concentrations of serotonin below the detection threshold. No serotonin observations were made in the second animal.

Supplementary Discussion

Future adjustments to the SPME neurochemical sensing. Several improvements to the protocol can be made in order to make SPME more informative. Using a more sensitive MS would reduce detection thresholds and increase sensitivity in detecting compounds not

successfully measured here such as GABA, serotonin or norepinephrine. This would be very impactful, especially in the case of Serotonin for reasons discussed above. Additionally, efforts could be made to improve the extracting phase synthesis and functionalization protocols and increase the extracting capabilities of SPME probes. Moreover, in order to decrease the MS background and interferences in the range of small molecules, derivatization strategy could be considered.

For GABA, the most promising strategy is post-desorption derivatization by reagent increasing the compound's hydrophobicity resulting in better MS signal such as benzoyl chloride (Wong 2016). Catecholamine and acetylcholine detection may be improved by optimizing the post-sampling analysis pipeline. Improvements can be made at several steps in order to better preserve and quantify catecholamines: (1) faster coupling of sampling to desorption (2) trying various antioxidant solutions and other preservatives for maintaining catecholamine integrity and (3) faster analysis of the desorbed analytes. Faster coupling of sampling to desorption could be achieved through a more stream-lined process of fibre placement and retraction involving a static cannula maintained through several sampling events. This mechanism would also allow for a faster replacement of SPME probes resulting in a shorter delay between consecutive measurements.

A preliminary experiment using spiked artificial cerebra-spinal fluid (aCSF) with very high, known concentrations of all target compounds yielded detectable concentrations of all target compounds indicating that the extracting phase of the SPME probe is capable of capturing all compounds of interest. Furthermore, simultaneously collected replicates displayed very little loss of collected compounds over several days when placed in a -80°C freezer (data not shown). Such findings neither support nor antagonize the suggested strategies for improving SPME yield and sensitivity in primates as detection properties within the aCSF do not seem to accurately reflect those observed in vivo in NHPs. This is likely contributed to by the dynamic and highly regulated nature of target compounds within the extracellular space of the brain and the dynamic equilibrium between the extracting phase of the SPME probes and the extracellular environment. Further tests of the possible differences between these two mediums and improvement strategies to SPME probes are subject for future studies.

Supplementary Figures

Fig S1. Experimental procedure from SPME probe fabrication to quantitation. Fabrication described the in-house procedure to prepare SPME probes. Preparation describes experimental set-up. Sampling describes the actual data collection process. LC/MS analysis describes the chemical quantitation of collected data samples.

Supplementary Tables

Table S1. Overview of in vivo neurochemical measurement methods

	PET imaging	**Electro-chemistry**	**Micro-dialysis**	**Solid phase micro-extraction**
Temporal Resolution	Minutes	Highest (millisecond range)	1-30 minutes (usually 20 minutes); dependent on MS sensitivity, target etc.	<5-30 minutes; dependent on MS sensitivity, coating thickness, target etc.
Spatial Resolution	Voxel	High; surface area may vary (relevant for enzyme based methods)	Diffusion based; surface area may vary	Diffusion based; surface area may vary
Sensitivity	Indirect measurement via competitive radiolabeled species	High	Depending on post-hoc methods (i.e. MS)	Depending on post-hoc methods (i.e. MS)
Neuro-active targets	A few at most	A few at most	Many	Many
Non-neuro-active targets	No	No	Yes, greater efficacy for hydrophilic compounds	Yes, greater potential efficacy for hydrophobic compounds
In vivo feasibility	Difficult in awake, behaving animal models; movement highly restricted	Good (low reliability in NHPs)	Good	Best
Cost	High	Requires special equipment	Requires special equipment	Easy to port to an acute micro-electrode setup; requires a chemistry core

Table S1. A comparison of methods capable of measuring single or multiple neurochemicals in vivo. Temporal resolution, spatial resolution, sensitivity, capability to measure neuro-active and non-neuro-active compounds, in vivo feasibility and cost. PET: positron emission tomography; NHP: non-human primate; MS: mass spectrometer.

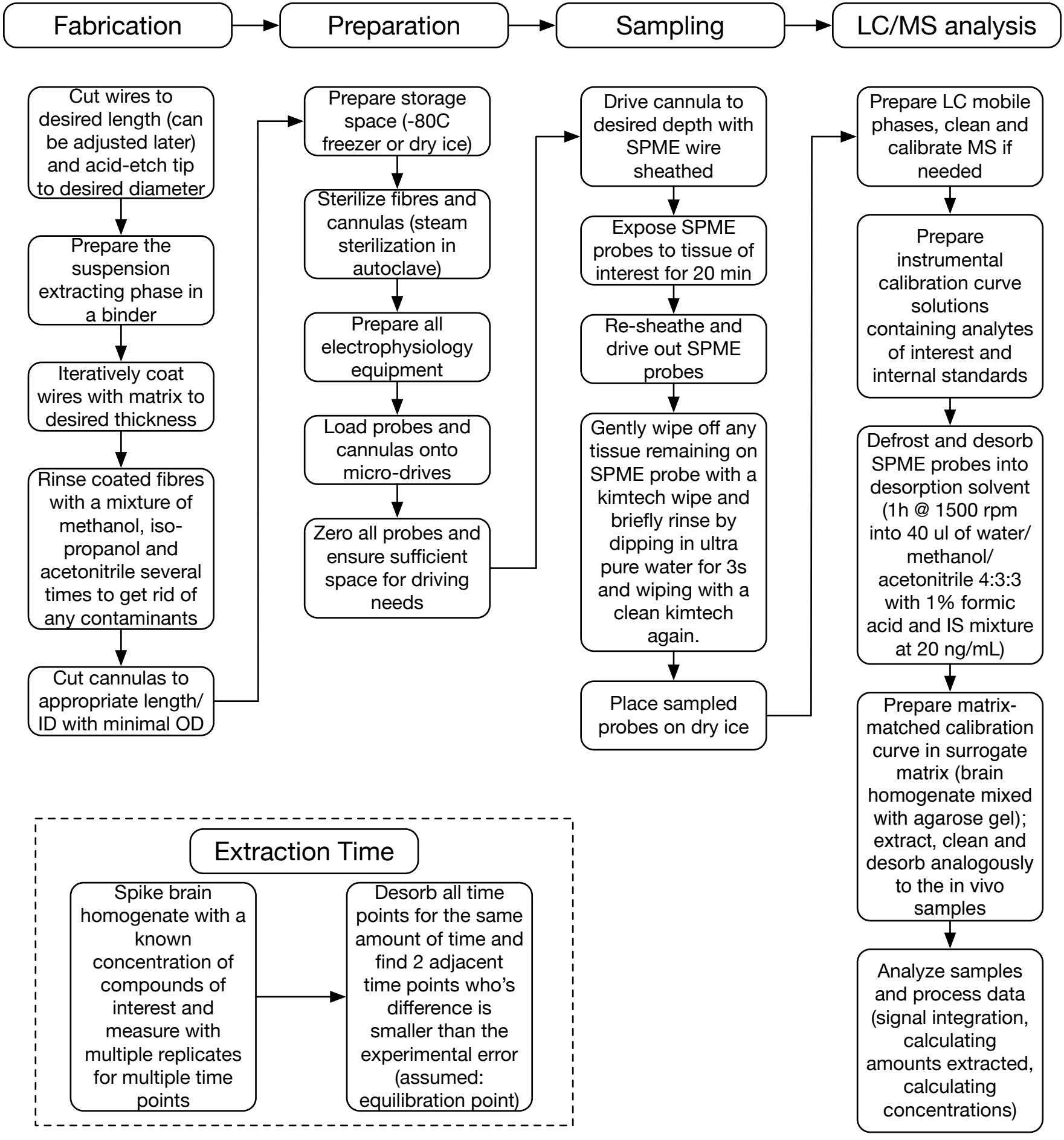
Fabrication
Preparation
Sampling
LC/MS analysis
Cut wires to desired length (can be adjusted later) and acid-etch tip to desired diameter
Prepare the suspension extracting phase in a binder
Iteratively coat wires with matrix to desired thickness
Rinse coated fibres with a mixture of methanol, iso-propanol and acetonitrile several times to get rid of any contaminants
Cut cannulas to appropriate length/ ID with minimal OD
Prepare storage space (-80C freezer or dry ice)
Sterilize fibres and cannulas (steam sterilization in autoclave)
Prepare all electrophysiology equipment
Load probes and cannulas onto micro-drives
Zero all probes and ensure sufficient space for driving needs
Drive cannula to desired depth with SPME wire sheathed
Expose SPME probes to tissue of interest for 20 min
Re-sheathe and drive out SPME probes
Gently wipe off any tissue remaining on SPME probe with a kimtech wipe and briefly rinse by dipping in ultra pure water for 3s and wiping with a clean kimtech again.
Place sampled probes on dry ice
Prepare LC mobile phases, clean and calibrate MS if needed
Prepare instrumental calibration curve solutions containing analytes of interest and internal standards
Defrost and desorb SPME probes into desorption solvent (1h @ 1500 rpm into 40 ul of water/ methanol/ acetonitrile 4:3:3 with 1% formic acid and IS mixture at 20 ng/mL)
Prepare matrix-matched calibration curve in surrogate matrix (brain homogenate mixed with agarose gel); extract, clean and desorb analogously to the in vivo samples
Analyze samples and process data (signal integration, calculating amounts extracted, calculating concentrations)
Extraction Time
Spike brain homogenate with a known concentration of compounds of interest and measure with multiple replicates for multiple time points
Desorb all time points for the same amount of time and find 2 adjacent time points who's difference is smaller than the experimental error (assumed: equilibration point)